

Supporting Information

Impact of flexible hexyl chain ordering in a mononuclear spin crossover iron(III) complex

Hiroaki Hagiwara,* and Kento Sonoda

Department of Chemistry, Faculty of Education, Gifu University, Yanagido 1-1, Gifu 501-1193, Japan

Table of Contents

Fig. S1 TG/DTA curve of [Fe(Hex-tnal) ₂]BPh ₄ (1)	S2
Fig. S2 IR spectrum (KBr) of 1 at room temperature (RT)	S2
Fig. S3 Experimental PXRD pattern of 1 at RT with the one calculated from the single-crystal X-ray data at 296 K	S3
Fig. S4 Temperature dependence of the $\chi_M T$ product over two consecutive thermal cycles for 1 at a sweep rate of 2 K min ⁻¹ .	S3
Fig. S5 DSC curves of 1 collected in the cooling and heating modes at different scan rates (2, 5, 8, and 10 K min ⁻¹)	S4
Table S1. Peak top temperatures of the DSC curves for 1 at different scan rates	S4
Table S2. X-ray crystallographic data for 1	S5
Table S3. Relevant coordination bond lengths (Å), angles (°), and structural parameters of 1	S6
Fig. S6 Temperature dependence of the HS molar fraction (γ_{HS}) of 1 obtained from the magnetic susceptibility measurements, average Fe–N/O coordination bond length, and octahedral volume	S7
Table S4. Atomic occupancy of C atoms (part A) of <i>n</i> -hexyl groups for 1	S7
Table S5. Definition of centroids (Cg) for aromatic rings of 1	S8
Table S6. Intermolecular Cg...Cg distances (Å) of 1	S9–10
Table S7. Intermolecular CH...O contacts of 1	S11
Table S8. Intermolecular CH... π hydrogen bond geometries of 1	S12
References	S13

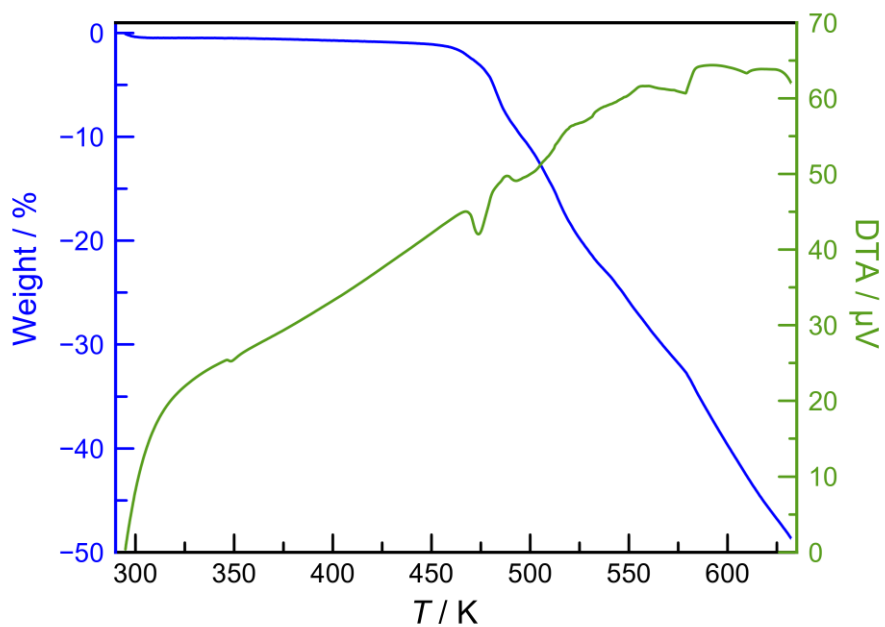


Fig. S1 TG/DTA curve of $[\text{Fe}(\text{Hex-tnal})_2]\text{BPh}_4$ (**1**).

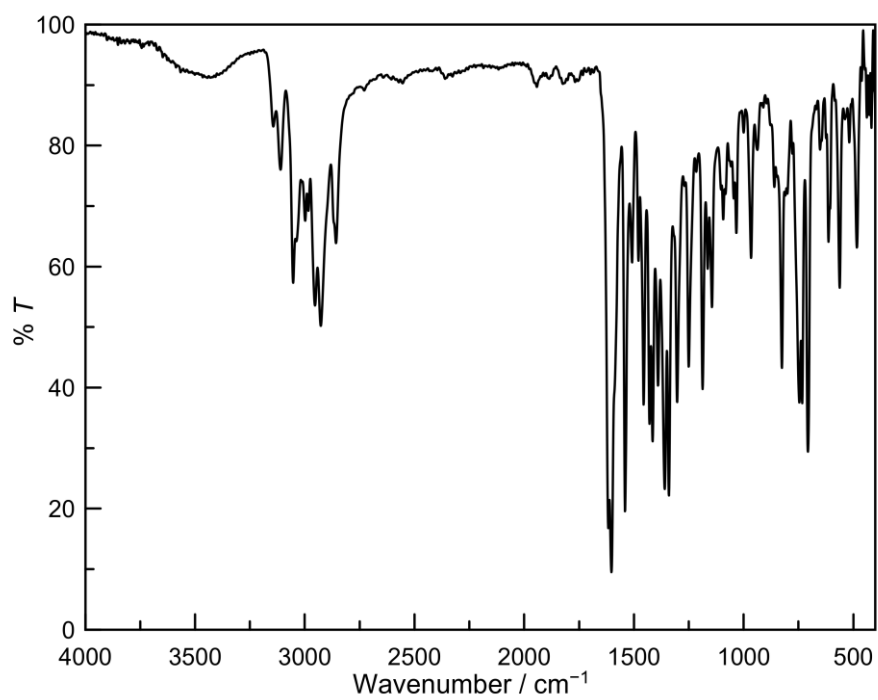


Fig. S2 IR spectrum (KBr) of **1** at room temperature (RT).

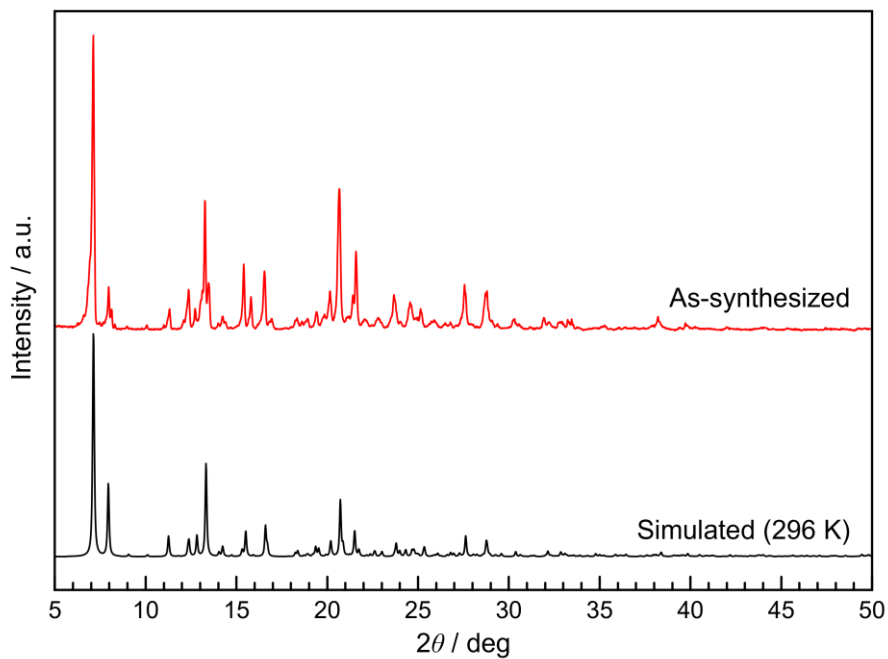


Fig. S3 Experimental PXR pattern of **1** (red) at RT with the one calculated from the single-crystal X-ray data at 296 K (gray).

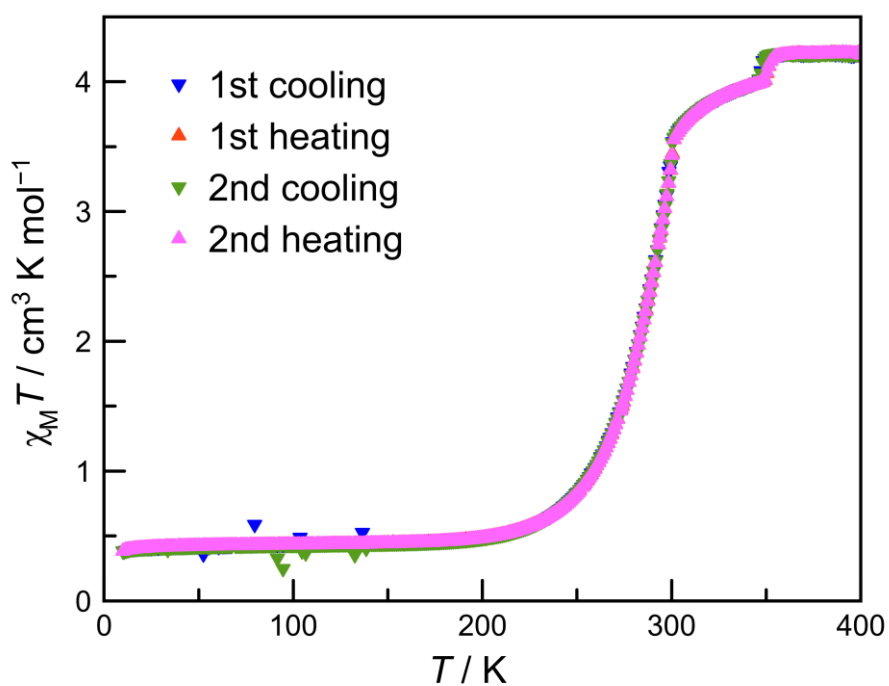


Fig. S4 Temperature dependence of the $\chi_M T$ product over two consecutive thermal cycles for **1** at a sweep rate of 2 K min^{-1} .

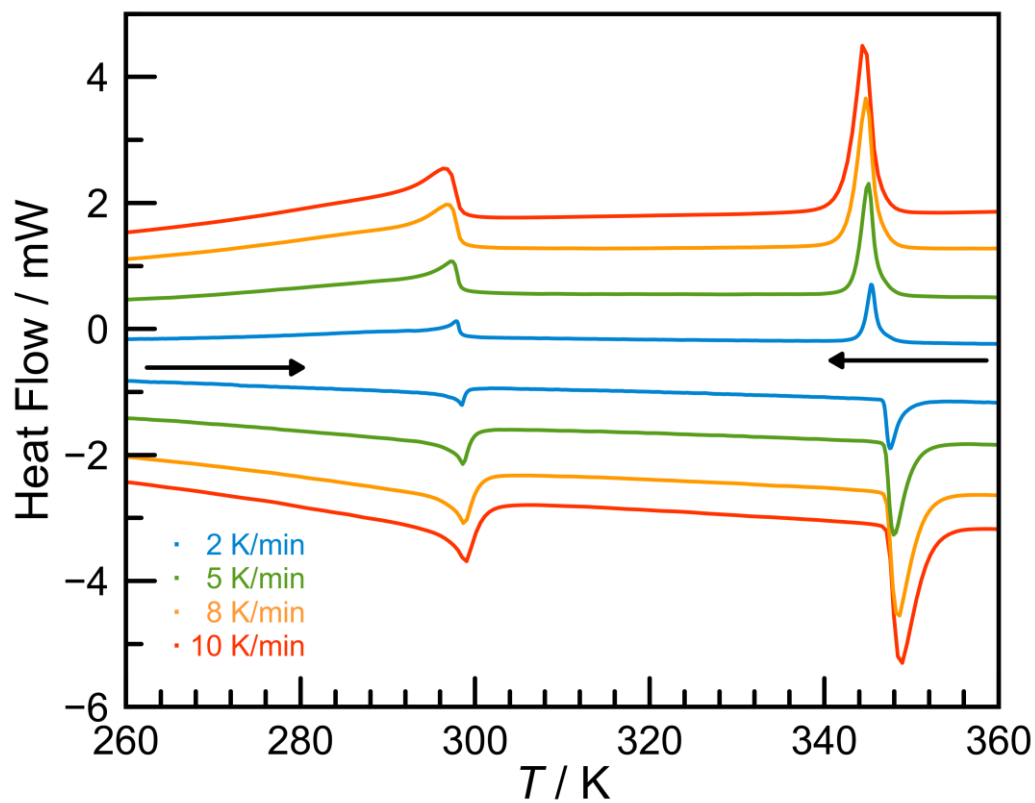


Fig. S5 DSC curves of **1** collected in the cooling and heating modes at different scan rates (2, 5, 8, and 10 K min⁻¹).

Table S1. Peak top temperatures of the DSC curves for **1** at different scan rates

Scan rate, K min ⁻¹	$T_{c1\downarrow}$, K	$T_{c1\uparrow}$, K	$T_{c2\downarrow}$, K	$T_{c2\uparrow}$, K
2	298	298	345	347
5	297	298	344	347
8	295	298	344	348
10	295	299	344	348

Table S2. X-ray crystallographic data for **1**

<i>T</i> , K	100	175	250	275	296	310	325	340	360
Formula	C ₆₄ H ₆₆ BFeN ₈ O ₂								
Formula weight	1045.90								
Crystal system	Triclinic	Triclinic	Triclinic	Triclinic	Monoclinic	Monoclinic	Monoclinic	Monoclinic	Triclinic
Space group	<i>P</i> $\bar{1}$	<i>P</i> $\bar{1}$	<i>P</i> $\bar{1}$	<i>P</i> $\bar{1}$	<i>C</i> 2/ <i>c</i>	<i>C</i> 2/ <i>c</i>	<i>C</i> 2/ <i>c</i>	<i>C</i> 2/ <i>c</i>	<i>P</i> $\bar{1}$
<i>a</i> , Å	14.2177(4)	14.2646(3)	14.3314(4)	14.3772(4)	14.8678(6)	14.8931(6)	14.9017(6)	14.9243(7)	13.9178(3)
<i>b</i> , Å	14.4364(4)	14.5053(3)	14.6187(5)	14.6177(5)	24.8747(9)	24.8823(9)	24.8537(9)	24.8378(10)	14.1124(3)
<i>c</i> , Å	15.8796(4)	15.9520(2)	16.0247(3)	16.1449(3)	16.3510(5)	16.3989(5)	16.4274(5)	16.4756(5)	17.1203(3)
α , deg	75.742(3)	75.861(2)	98.737(2)	98.821(2)	90	90	90	90	96.939(2)
β , deg	85.560(2)	84.957(2)	95.692(2)	96.291(2)	106.187(4)	106.285(4)	106.331(4)	106.339(4)	98.241(2)
γ , deg	61.152(3)	60.854(2)	119.179(3)	118.781(3)	90	90	90	90	115.296(2)
<i>V</i> , Å ³	2763.62(15)	2793.53(10)	2838.25(16)	2872.06(16)	5807.4(4)	5833.2(4)	5838.6(4)	5860.6(4)	2945.89(11)
<i>Z</i>	2	2	2	2	4	4	4	4	2
<i>T</i> , K	100(2)	175(2)	250(2)	275(2)	296(2)	310(2)	325(2)	340(2)	360(2)
μ (Mo K α), mm ⁻¹	0.325	0.322	0.317	0.313	0.310	0.308	0.308	0.307	0.305
<i>d</i> _{calcd.} , g cm ⁻³	1.257	1.243	1.224	1.209	1.196	1.191	1.190	1.185	1.179
Reflections collected	23406	24767	25421	25823	25309	25336	25461	25526	25263
Independent reflections	14467	14789	15085	15240	8018	8032	8052	8084	15492
<i>R</i> _{int}	0.0170	0.0155	0.0188	0.0225	0.0166	0.0169	0.0167	0.0172	0.0108
<i>R</i> ₁ ^a (<i>I</i> > 2 σ (<i>I</i>))	0.0563	0.0622	0.0612	0.0690	0.0501	0.0484	0.0487	0.0500	0.0555
<i>R</i> ₁ ^a (all data)	0.0669	0.0744	0.0830	0.0977	0.0675	0.0663	0.0694	0.0750	0.0763
w <i>R</i> ₂ ^b (<i>I</i> > 2 σ (<i>I</i>))	0.1545	0.1641	0.1603	0.1928	0.1389	0.1356	0.1338	0.1366	0.1594
w <i>R</i> ₂ ^b (all data)	0.1602	0.1705	0.1726	0.2126	0.1521	0.1488	0.1496	0.1550	0.1803
<i>S</i>	1.129	1.154	1.103	1.091	1.042	1.048	1.027	1.023	1.036
CCDC number	2331987	2331988	2331989	2331990	2331991	2331992	2331993	2331994	2331995

^a $R_1 = \sum ||F_o| - |F_c|| / \sum |F_o|$.

^b $wR_2 = [\sum w(|F_o|^2 - |F_c|^2)^2 / \sum w|F_o|^2]^{1/2}$.

Table S3. Relevant coordination bond lengths (Å), angles (°), and structural parameters of **1**

<i>T</i> , K	100	175	250	275	296	310	325	340	360
	Bond Lengths (Å)								
Fe1–O1	1.8720(16)	1.8707(18)	1.8688(17)	1.876(2)	1.9025(13)	1.9045(12)	1.9053(12)	1.9053(13)	1.9095(14)
Fe1–O2 (Fe1–O1*) ^a	1.8789(16)	1.8767(17)	1.8719(17)	1.877(2)	1.9026(13)	1.9045(12)	1.9052(12)	1.9054(13)	1.9080(15)
Fe1–N3	1.9481(19)	1.949(2)	1.969(2)	2.018(2)	2.0955(15)	2.1065(14)	2.1114(15)	2.1178(15)	2.1531(17)
Fe1–N4	1.9347(18)	1.940(2)	1.9498(18)	2.002(2)	2.0862(13)	2.0950(12)	2.1002(12)	2.1044(13)	2.1060(14)
Fe1–N7 (Fe1–N3*) ^a	1.9525(19)	1.951(2)	1.9676(19)	2.016(2)	2.0956(15)	2.1065(14)	2.1115(15)	2.1179(15)	2.1436(18)
Fe1–N8 (Fe1–N4*) ^a	1.9363(18)	1.9393(19)	1.9473(18)	1.996(2)	2.0862(13)	2.0951(12)	2.1003(12)	2.1044(13)	2.1159(15)
Average Fe–O (Fe–O _{ave})	1.875	1.874	1.870	1.877	1.903	1.905	1.905	1.905	1.909
Average Fe–N (Fe–N _{ave})	1.943	1.945	1.958	2.008	2.091	2.101	2.106	2.111	2.130
Average Fe–N/O (Fe–N/O _{ave})	1.920	1.921	1.929	1.964	2.028	2.035	2.039	2.043	2.056
	Bond Angles (deg)								
O1–Fe1–O2 (O1–Fe1–O1*) ^a	95.03(7)	94.95(8)	95.33(8)	96.49(9)	97.96(8)	98.13(8)	98.21(8)	98.31(9)	98.40(7)
O1–Fe1–N3	172.35(7)	172.32(8)	171.23(8)	167.85(9)	162.24(5)	161.67(5)	161.31(5)	160.96(6)	161.15(6)
O1–Fe1–N4	93.42(7)	93.44(8)	92.68(8)	90.72(9)	86.81(5)	86.46(5)	86.25(5)	86.04(5)	85.83(6)
O1–Fe1–N7 (O1–Fe1–N3*) ^a	90.31(7)	90.28(8)	90.20(8)	90.37(10)	91.61(6)	91.71(6)	91.79(6)	91.88(6)	92.04(7)
O1–Fe1–N8 (O1–Fe1–N4*) ^a	86.71(7)	87.06(8)	88.13(8)	91.12(9)	97.29(5)	97.83(5)	98.18(5)	98.52(5)	97.16(6)
O2–Fe1–N3 (O1*–Fe1–N3) ^a	91.10(7)	91.04(8)	91.03(8)	91.21(10)	91.61(6)	91.71(6)	91.80(6)	91.88(6)	91.22(7)
O2–Fe1–N4 (O1*–Fe1–N4) ^a	88.67(7)	88.45(8)	89.13(8)	92.05(9)	97.29(5)	97.83(5)	98.18(5)	98.52(5)	103.79(6)
O2–Fe1–N7 (O1*–Fe1–N3*) ^a	172.36(7)	172.51(8)	171.54(8)	168.25(9)	162.24(5)	161.67(5)	161.31(5)	160.96(6)	159.51(6)
O2–Fe1–N8 (O1*–Fe1–N4*) ^a	92.36(7)	92.54(8)	92.14(7)	90.44(9)	86.81(5)	86.46(5)	86.25(5)	86.04(5)	85.48(6)
N3–Fe1–N4	82.12(8)	81.90(8)	81.36(8)	79.59(9)	77.12(5)	76.87(5)	76.68(5)	76.53(6)	76.11(6)
N3–Fe1–N7 (N3–Fe1–N3*) ^a	84.05(8)	84.23(9)	84.19(8)	83.70(10)	83.36(9)	83.30(9)	83.27(9)	83.19(9)	84.13(7)
N3–Fe1–N8 (N3–Fe1–N4*) ^a	97.64(8)	97.49(8)	97.68(8)	98.23(9)	98.16(6)	98.19(5)	98.19(5)	98.19(6)	99.74(7)
N4–Fe1–N7 (N4–Fe1–N3*) ^a	96.47(8)	96.61(8)	97.02(8)	97.40(9)	98.16(6)	98.19(5)	98.19(5)	98.19(6)	94.47(7)
N4–Fe1–N8 (N4–Fe1–N4*) ^a	178.95(8)	178.86(8)	178.43(8)	176.72(9)	173.78(8)	173.49(7)	173.26(7)	173.07(8)	169.79(7)
N7–Fe1–N8 (N3*–Fe1–N4*) ^a	82.48(8)	82.36(8)	81.63(8)	79.87(9)	77.12(5)	76.87(5)	76.68(5)	76.53(6)	75.72(7)
Σ^b	52.31	52.35	51.64	54.86	80.86	83.63	85.43	87.17	89.54
Θ^c	150.79	150.71	160.15	191.05	254.42	261.38	265.96	269.92	291.42
Octahedral volume (V_{Oh}) ^d	9.325	9.333	9.442	9.926	10.804	10.902	10.950	10.996	11.176

Symmetry operation: (*), 1–X, Y, 3/2–Z.

^a The label in parentheses indicates the data at 296, 310, 325, and 340 K.^b Σ = the sum of $|90 - \phi|$ for the 12 *cis* N/O–Fe–N/O angles in the octahedral coordination sphere^{S1} calculated using the program OctaDist.^{S2}^c Θ = the sum of $|60 - \theta|$ for the 24 N/O–Fe–N/O angles describing the trigonal twist angles^{S3} calculated using the program OctaDist.^{S2}^d Calculated using the program OLEX2.^{S4}

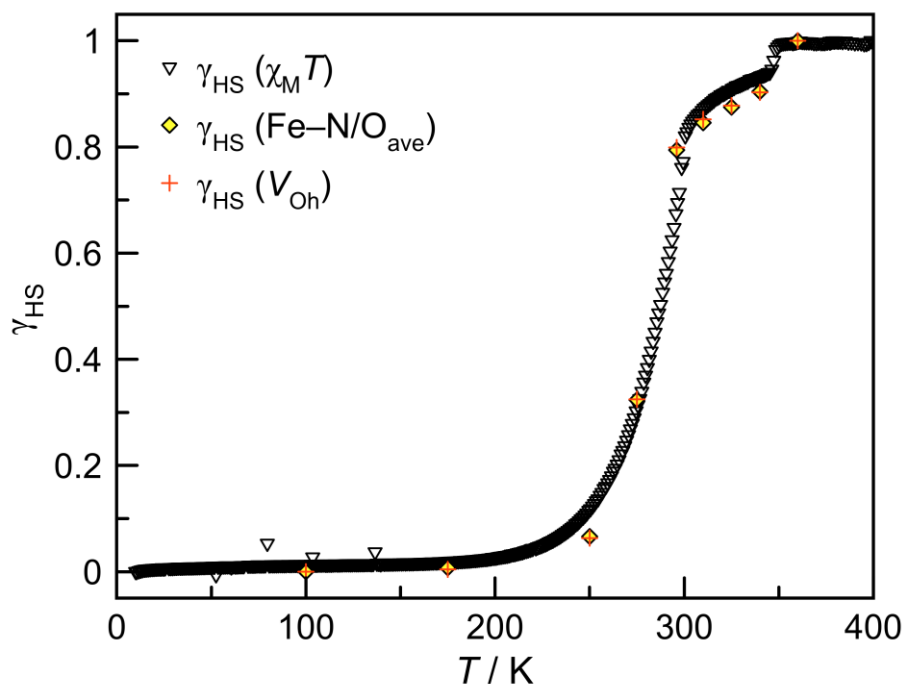


Fig. S6 Temperature dependence of the HS molar fraction (γ_{HS}) of **1** obtained from the magnetic susceptibility measurements (black inverted triangles), average Fe–N/O coordination bond length (Fe–N/O_{ave}, yellow diamonds), and octahedral volume (V_{Oh} , red cross).

Table S4. Atomic occupancy of C atoms (part A) of *n*-hexyl groups for **1**

<i>T</i> , K	100	175	250	275	296	310	325	340	360
C1A	n/a	n/a	n/a	n/a	0.653(5)	0.658(5)	0.663(5)	0.653(5)	n/a
C2A	n/a	n/a	n/a	n/a	0.653(5)	0.658(5)	0.663(5)	0.653(5)	n/a
C3A	n/a	n/a	0.497(8)	0.645(12)	0.653(5)	0.658(5)	0.663(5)	0.653(5)	n/a
C1A ^{*,a}	n/a	n/a	n/a	n/a	0.653(5)	0.658(5)	0.663(5)	0.653(5)	n/a
C2A ^{*,a}	n/a	n/a	n/a	n/a	0.653(5)	0.658(5)	0.663(5)	0.653(5)	n/a
C3A ^{*,a}	n/a	n/a	n/a	n/a	0.653(5)	0.658(5)	0.663(5)	0.653(5)	n/a
C21A	n/a	n/a	0.717(7)	0.726(10)	n/a	n/a	n/a	n/a	n/a
C22A	n/a	n/a	0.717(7)	0.726(10)	n/a	n/a	n/a	n/a	n/a
C23A	n/a	0.742(5)	n/a	n/a	n/a	n/a	n/a	n/a	n/a
C24A	n/a	0.742(5)	0.599(5)	0.585(6)	n/a	n/a	n/a	n/a	n/a
C25A	n/a	0.742(5)	0.599(5)	0.585(6)	n/a	n/a	n/a	n/a	n/a

Symmetry operation: (*), 1–X, Y, 3/2–Z.

^a At 296, 310, 325, and 340 K.

Table S5. Definition of centroids (Cg) for aromatic rings of **1^{S5}**

<i>T</i> , K	Component	Ring	Ring size	Centroid	Related atoms	
100, 360	Cation	Chelate	5-Membered	Cg1	Fe1–N3–C8–C9–N4	
		Chelate	5-Membered	Cg2	Fe1–N7–C28–C29–N8	
		Triazolyl	5-Membered	Cg3	N1–N2–N3–C8–C7	
		Triazolyl	5-Membered	Cg4	N5–N6–N7–C28–C27	
		Chelate	6-Membered	Cg5	Fe1–O1–C20–C11–C10–N4	
		Chelate	6-Membered	Cg6	Fe1–O2–C40–C31–C30–N8	
		Naphthyl	6-Membered	Cg7	C11–C12–C17–C18–C19–C20	
		Naphthyl	6-Membered	Cg8	C12–C13–C14–C15–C16–C17	
		Naphthyl	6-Membered	Cg9	C31–C32–C37–C38–C39–C40	
		Naphthyl	6-Membered	Cg10	C32–C33–C34–C35–C36–C37	
		Naphthyl	10-Membered	Cg11	C11–C12–C13–C14–C15–C16–C17–C18–C19–C20	
		Naphthyl	10-Membered	Cg12	C31–C32–C33–C34–C35–C36–C37–C38–C39–C40	
	Anion	Phenyl	6-Membered	Cg13	C41–C42–C43–C44–C45–C46	
		Phenyl	6-Membered	Cg14	C47–C48–C49–C50–C51–C52	
		Phenyl	6-Membered	Cg15	C53–C54–C55–C56–C57–C58	
		Phenyl	6-Membered	Cg16	C59–C60–C61–C62–C63–C64	
175, 250, 275	Cation	Chelate	5-Membered	Cg1	Fe1–N3–C8–C9–N4	
		Chelate	5-Membered	Cg2	Fe1–N7–C28–C29–N8	
		Triazolyl	5-Membered	Cg3	N1–N2–N3–C8–C7	
		Triazolyl	5-Membered	Cg4	N5–N6–N7–C28–C27	
		Chelate	6-Membered	Cg5	Fe1–O1–C20–C11–C10–N4	
		Chelate	6-Membered	Cg6	Fe1–O2–C40–C31–C30–N8	
		Naphthyl	6-Membered	Cg7	C11–C12–C17–C18–C19–C20	
		Naphthyl	6-Membered	Cg8	C12–C13–C14–C15–C16–C17	
		Naphthyl	6-Membered	Cg9	C31–C32–C37–C38–C39–C40	
		Naphthyl	6-Membered	Cg10	C32–C33–C34–C35–C36–C37	
		Anion	Phenyl	6-Membered	Cg11	C41–C42–C43–C44–C45–C46
			Phenyl	6-Membered	Cg12	C47–C48–C49–C50–C51–C52
	Phenyl		6-Membered	Cg13	C53–C54–C55–C56–C57–C58	
	Phenyl		6-Membered	Cg14	C59–C60–C61–C62–C63–C64	
	296, 310, 325, 340	Cation	Chelate	5-Membered	Cg1	Fe1–N3–C8–C9–N4
			Chelate	5-Membered	Cg2	Fe1–N3*–C8*–C9*–N4*
Triazolyl			5-Membered	Cg3	N1–N2–N3–C8–C7	
Chelate			6-Membered	Cg4	Fe1–O1–C20–C11–C10–N4	
Chelate			6-Membered	Cg5	Fe1–O1*–C20*–C11*–C10*–N4*	
Naphthyl			6-Membered	Cg6	C11–C12–C17–C18–C19–C20	
Naphthyl			6-Membered	Cg7	C12–C13–C14–C15–C16–C17	
Anion		Phenyl	6-Membered	Cg8	C21–C22–C23–C24–C25–C26	
		Phenyl	6-Membered	Cg9	C27–C28–C29–C30–C31–C32	

Symmetry operation: (*), 1–X, Y, 3/2–Z.

Table S6. Intermolecular Cg \cdots Cg distances (Å) of **1**

<i>T</i> , K	$\pi\cdots\pi$	Cg \cdots Cg, Å	Symmetry code
100	Cg3 \cdots Cg13	3.4974(16)	X, Y, Z
	Cg4 \cdots Cg15	3.5927(14)	X, 1+Y, Z
	Cg7 \cdots Cg8	3.7245(18)	-X, 2-Y, 1-Z
	Cg8 \cdots Cg7	3.7245(18)	-X, 2-Y, 1-Z
	Cg8 \cdots Cg8	3.4927(16)	-X, 2-Y, 1-Z
	Cg9 \cdots Cg10 ^a	4.3345(14)	-X, 2-Y, 2-Z
	Cg10 \cdots Cg9 ^a	4.3346(14)	-X, 2-Y, 2-Z
	Cg10 \cdots Cg10	3.5818(14)	-X, 2-Y, 2-Z
	Cg13 \cdots Cg3	3.4975(16)	X, Y, Z
	Cg15 \cdots Cg4	3.5928(14)	X, -1+Y, Z
175	Cg3 \cdots Cg11	3.5179(19)	X, Y, Z
	Cg4 \cdots Cg13	3.6148(17)	X, 1+Y, Z
	Cg7 \cdots Cg8	3.777(2)	-X, 2-Y, 1-Z
	Cg8 \cdots Cg7	3.777(2)	-X, 2-Y, 1-Z
	Cg8 \cdots Cg8	3.493(2)	-X, 2-Y, 1-Z
	Cg9 \cdots Cg10 ^a	4.2677(17)	-X, 2-Y, 2-Z
	Cg10 \cdots Cg9 ^a	4.2677(17)	-X, 2-Y, 2-Z
	Cg10 \cdots Cg10	3.5718(18)	-X, 2-Y, 2-Z
	Cg11 \cdots Cg3	3.5179(19)	X, Y, Z
	Cg13 \cdots Cg4	3.6149(17)	X, -1+Y, Z
250	Cg3 \cdots Cg11	3.553(2)	X, Y, Z
	Cg4 \cdots Cg13	3.6702(18)	-1+X, -1+Y, Z
	Cg7 \cdots Cg8	3.829(3)	1-X, -Y, 1-Z
	Cg8 \cdots Cg7	3.829(3)	1-X, -Y, 1-Z
	Cg8 \cdots Cg8	3.513(2)	1-X, -Y, 1-Z
	Cg9 \cdots Cg10 ^a	4.2192(17)	1-X, -Y, 2-Z
	Cg10 \cdots Cg9 ^a	4.2192(17)	1-X, -Y, 2-Z
	Cg10 \cdots Cg10	3.5725(18)	1-X, -Y, 2-Z
	Cg11 \cdots Cg3	3.553(2)	X, Y, Z
	Cg13 \cdots Cg4	3.6702(18)	1+X, 1+Y, Z
275	Cg3 \cdots Cg11	3.565(2)	X, Y, Z
	Cg4 \cdots Cg13	3.690(2)	-1+X, -1+Y, Z
	Cg7 \cdots Cg8	3.812(3)	1-X, -Y, 1-Z
	Cg8 \cdots Cg7	3.812(3)	1-X, -Y, 1-Z
	Cg8 \cdots Cg8	3.560(3)	1-X, -Y, 1-Z
	Cg9 \cdots Cg10	4.115(2)	1-X, -Y, 2-Z
	Cg10 \cdots Cg9	4.115(2)	1-X, -Y, 2-Z
	Cg10 \cdots Cg10	3.580(2)	1-X, -Y, 2-Z
	Cg11 \cdots Cg3	3.565(2)	X, Y, Z
	Cg13 \cdots Cg4	3.690(2)	1+X, 1+Y, Z

^a The Cg \cdots Cg distance is slightly longer than the typical value of $\pi\cdots\pi$ stacking interaction.

Table S6. Intermolecular Cg \cdots Cg distances (Å) of **1** (continue)

<i>T</i> , K	$\pi\cdots\pi$	Cg \cdots Cg, Å	Symmetry code
296	Cg3 \cdots Cg8	3.6238(17)	X, Y, Z
	Cg6 \cdots Cg7	3.8247(15)	1-X, -Y, 1-Z
	Cg7 \cdots Cg6	3.8247(15)	1-X, -Y, 1-Z
	Cg7 \cdots Cg7	3.6381(14)	1-X, -Y, 1-Z
	Cg8 \cdots Cg3	3.6239(17)	X, Y, Z
310	Cg3 \cdots Cg8	3.6290(17)	X, Y, Z
	Cg6 \cdots Cg7	3.8247(14)	1-X, -Y, 1-Z
	Cg7 \cdots Cg6	3.8247(14)	1-X, -Y, 1-Z
	Cg7 \cdots Cg7	3.6557(13)	1-X, -Y, 1-Z
	Cg8 \cdots Cg3	3.6290(17)	X, Y, Z
325	Cg3 \cdots Cg8	3.6316(17)	X, Y, Z
	Cg6 \cdots Cg7	3.8232(14)	1-X, -Y, 1-Z
	Cg7 \cdots Cg6	3.8232(14)	1-X, -Y, 1-Z
	Cg7 \cdots Cg7	3.6681(13)	1-X, -Y, 1-Z
	Cg8 \cdots Cg3	3.6316(17)	X, Y, Z
340	Cg3 \cdots Cg8	3.6374(19)	X, Y, Z
	Cg6 \cdots Cg7	3.8245(15)	1-X, -Y, 1-Z
	Cg7 \cdots Cg6	3.8244(15)	1-X, -Y, 1-Z
	Cg7 \cdots Cg7	3.6813(14)	1-X, -Y, 1-Z
	Cg8 \cdots Cg3	3.6375(19)	X, Y, Z
360	Cg3 \cdots Cg13	4.128(2)	X, Y, Z
	Cg4 \cdots Cg15	3.7417(17)	-1+X, -1+Y, Z
	Cg7 \cdots Cg8	3.7000(16)	1-X, -Y, 1-Z
	Cg8 \cdots Cg7	3.7000(16)	1-X, -Y, 1-Z
	Cg8 \cdots Cg8	3.7531(14)	1-X, -Y, 1-Z
	Cg9 \cdots Cg10	3.9641(16)	1-X, -Y, 2-Z
	Cg10 \cdots Cg9	3.9640(16)	1-X, -Y, 2-Z
	Cg10 \cdots Cg10 ^a	4.2545(16)	1-X, -Y, 2-Z
	Cg13 \cdots Cg3	4.128(2)	X, Y, Z
Cg15 \cdots Cg4	3.7417(17)	1+X, 1+Y, Z	

^a The Cg \cdots Cg distance is slightly longer than the typical value of $\pi\cdots\pi$ stacking interaction.

Table S7. Intermolecular CH \cdots O contacts of **1**

<i>T</i> , K	C–H \cdots X	H \cdots X, Å	C \cdots X, Å	C–H \cdots X, °	Symmetry code
100	C15–H15 \cdots O2	2.60	3.495(4)	158	–X, 2–Y, 1–Z
	C35–H35 \cdots O1 ^a	3.060	3.935(3) ^a	154	
175	C15–H15 \cdots O2	2.64	3.537(4)	159	–X, 2–Y, 1–Z
	C35–H35 \cdots O1 ^a	3.051	3.932(3)	155	
250	C15–H15 \cdots O2	2.70	3.590(5)	159	1–X, –Y, 1–Z
	C35–H35 \cdots O1 ^a	3.059	3.933(5)	155	
275	C15–H15 \cdots O2	2.71	3.596(7)	159	1–X, –Y, 1–Z
	C35–H35 \cdots O1	2.988	3.862(6)	157	
296	C15–H15 \cdots O1	2.74	3.625(3)	158	X, –Y, –1/2+Z
310	C15–H15 \cdots O1	2.75	3.628(3)	158	X, –Y, –1/2+Z
325	C15–H15 \cdots O1	2.75	3.628(3)	158	X, –Y, –1/2+Z
340	C15–H15 \cdots O1	2.76	3.635(3)	157	X, –Y, –1/2+Z
360	C15–H15 \cdots O2	2.65	3.531(4)	158	1–X, –Y, 1–Z
	C35–H35 \cdots O1	2.79	3.573(4)	143	1–X, –Y, 2–Z

^a The contact distance is slightly longer than the typical value of C–H \cdots O hydrogen bond.

Table S8. Intermolecular CH $\cdots\pi$ hydrogen bond geometries of **1**

<i>T</i> , K	C–H $\cdots\pi$	H \cdots Cg, Å	C \cdots Cg, Å	C–H \cdots Cg, °	Symmetry code
100	C4–H4B \cdots Cg3	3.00	3.634(3)	123	X, Y, Z
	C7–H7 \cdots Cg14	2.55	3.467(3)	163	X, Y, Z
	C25–H25B \cdots Cg8	2.68	3.620(3)	159	1–X, 2–Y, 1–Z
	C25–H25B \cdots Cg11	2.62	3.561(3)	159	1–X, 2–Y, 1–Z
	C27–H27 \cdots Cg16	2.38	3.328(3)	179	X, 1+Y, Z
	C33–H33 \cdots Cg16	2.82	3.673(3)	150	1–X, 1–Y, 2–Z
175	C7–H7 \cdots Cg12	2.54	3.465(3)	165	X, Y, Z
	C25A–H25A \cdots Cg8	2.72	3.656(6)	157	1–X, 2–Y, 1–Z
	C27–H27 \cdots Cg14	2.40	3.351(3)	177	X, 1+Y, Z
	C33–H33 \cdots Cg14	2.86	3.713(3)	150	1–X, 1–Y, 2–Z
	C25B–H25C \cdots Cg7	2.72	3.638(14)	154	1–X, 2–Y, 1–Z
250	C7–H7 \cdots Cg12	2.55	3.476(3)	167	X, Y, Z
	C25A–H25A \cdots Cg8	2.77	3.687(8)	155	–X, –Y, 1–Z
	C27–H27 \cdots Cg14	2.45	3.391(3)	175	–1+X, –1+Y, Z
	C33–H33 \cdots Cg14	2.92	3.776(4)	152	1–X, 1–Y, 2–Z
	C25B–H25C \cdots Cg7	2.74	3.651(11)	155	–X, –Y, 1–Z
275	C7–H7 \cdots Cg12	2.57	3.484(4)	168	X, Y, Z
	C25A–H25A \cdots Cg8	2.82	3.724(10)	156	–X, –Y, 1–Z
	C27–H27 \cdots Cg14	2.49	3.413(5)	175	–1+X, –1+Y, Z
	C33–H33 \cdots Cg14	2.96	3.813(5)	152	1–X, 1–Y, 2–Z
296	C25B–H25C \cdots Cg7	2.73	3.637(13)	156	–X, –Y, 1–Z
	C5–H5A \cdots Cg6	2.97	3.855(7)	152	1/2+X, 1/2–Y, 1/2+Z
	C7–H7 \cdots Cg9	2.54	3.456(3)	170	X, Y, Z
	C2B–H2BB \cdots Cg8	2.99	3.77(3)	138	3/2–X, 1/2–Y, 2–Z
310	C5–H5A \cdots Cg6	2.98	3.863(7)	152	1/2+X, 1/2–Y, 1/2+Z
	C7–H7 \cdots Cg9	2.55	3.464(3)	170	X, Y, Z
	C2B–H2BB \cdots Cg8	2.98	3.79(3)	142	3/2–X, 1/2–Y, 2–Z
325	C5–H5A \cdots Cg6	2.97	3.865(7)	153	1/2+X, 1/2–Y, 1/2+Z
	C7–H7 \cdots Cg9	2.55	3.471(3)	170	X, Y, Z
340	C5–H5A \cdots Cg6	2.97	3.874(7)	155	1/2+X, 1/2–Y, 1/2+Z
	C7–H7 \cdots Cg9	2.57	3.485(3)	170	X, Y, Z
360	C5–H5B \cdots Cg12	2.90	3.823(7)	158	1–X, 1–Y, 2–Z
	C7–H7 \cdots Cg14	2.87	3.748(3)	158	X, Y, Z
	C13–H13 \cdots Cg14	2.96	3.772(3)	146	1–X, 1–Y, 1–Z
	C27–H27 \cdots Cg16	2.68	3.587(3)	166	–1+X, –1+Y, Z

References

- S1 P. Guionneau, M. Marchivie, G. Bravic, J.-F. Létard and D. Chasseau, *Top. Curr. Chem.*, 2004, **234**, 97–128.
- S2 R. Ketkaew, Y. Tantirungrotechai, P. Harding, G. Chastanet, P. Guionneau, M. Marchivie and D. J. Harding, *Dalton Trans.*, 2021, **50**, 1086–1096.
- S3 M. Marchivie, P. Guionneau, J.-F. Létard and D. Chasseau, *Acta Crystallogr., Sect. B: Struct. Sci.*, 2005, **61**, 25–28.
- S4 O. V. Dolomanov, L. J. Bourhis, R. J. Gildea, J. A. K. Howard and H. Puschmann, *J. Appl. Crystallogr.*, 2009, **42**, 339–341.
- S5 A. L. Spek, PLATON, A multipurpose Crystallographic Tool, 2011, Utrecht University, Utrecht, The Netherlands: A. L. Spek, *Acta Cryst.*, 2009, **D65**, 148–155.